hep-ph/9610nnn

ISSN 0418-9833

DESY 96-218
October 1996

arXiv:hep-ph/9610398v1 17 Oct 1996

Deep Inelastic Physics with H1 [1]

Max Klein

DESY-Inst. f. Hochenergiephysik, Zeuthen
Platanenallee 6, D-15738 Zeuthen, Germany. klein@ifh.de

Abstract

A summary is presented of deep inelastic physics results obtained by the H1 collaboration during its first three years of experimentation at the electron-proton collider HERA.

[1] Invited talk held at the 4th International Conference on Deep Inelastic Scattering, Rome, April 1996

1 Introduction

About 20 years ago, at the time of the advent of asymptotically free field theories of strong interactions [1], the option was seriously considered of a high energy colliding electron-proton machine CHEEP [2] at CERN and also at most of the other big accelerator laboratories [3]. It then seemed "that hadrons contain quark-parton constitutents which are rather point-like and carry the weak and electromagnetic couplings of strongly interacting matter [4, 5]. The nucleon seems to contain other constitutents without these couplings, which one may call 'gluons' without any prejudice as to their nature" [6]. The quark-gluon interactions explored with virtual photons of large mass $Q^2 \geq M_p^2$ are the subject of present day deep inelastic physics. The Rome conference took place nearly 5 years after the first *ep* collisions were succesfully observed by the H1 and ZEUS experiments at HERA.

This report summarizes results reported to this conference by the H1 experiment [7]. The H1 Collaboration submitted 16 papers which were discussed during the parallel sessions. For the introduction of the opening session a choice had to be made in order to present a consistent review without preempting the individual contributions. This choice emphasized the classical deep inelastic physics subjects - structure functions, gluon distribution, α_s, charged currents and deep inelastic diffraction [8]- where H1 obtained important new results, compare [9].

The H1 Collaboration succeeded in presenting to the conference the first precision measurement [10] of the proton structure function $F_2(x, Q^2)$ with an error as small as 5% at $Q^2 \simeq 20$ GeV^2, the measurement range extending in Bjorken x from $3 \cdot 10^{-5}$ at $Q^2 = 1.5$ GeV^2 to $x = 0.32$ at $Q^2 = 5000$ GeV^2. This result is discussed in sect.2.

A salient feature of the HERA experiments H1 and ZEUS is their ability to reconstruct the complete hadronic final state besides the scattered lepton. This offers many complementary ways for precision tests of QCD. In particular, as discussed in sect.3, information on the gluon distribution $xg(x, Q^2)$ can be obtained in a wide range of x analyzing the observed scaling violations, the longitudinal structure function F_L, charm production *via* photon-gluon fusion, vector meson production and deep inelastic jet production.

HERA will permit a very precise determination of the strong coupling constant with a possible systematic error of $\delta\alpha_s(M_Z^2) \simeq 0.002$ [11] once its ambitious running program is approaching completion. Important steps towards this precision were presented to this conference, as discussed in sect.4, by establishing the running of $\alpha_s(Q^2)$ in DIS jet production, by precisely describing the F_2 scaling violations with a NLO DGLAP [12] QCD procedure, and by determining $\alpha_s(Q^2)$ in the double logarithmic scaling approximation of the low x and large Q^2 behaviour of F_2.

Due to the high Q^2 range accessible, the HERA collider enables the study of neutrino physics and the electroweak interaction in the spacelike region. Sect.5 presents the first results of H1, based on 130 charged current events with 6.4 pb^{-1} luminosity, probing the proton structure with virtual W bosons at large x.

Finally, sect.6 is devoted to hard diffraction events, those as described in 1987 [13] "in which the target proton emerges isolated in rapidity" and which "probe the quark and antiquark content of the pomeron, that is they measure the pomeron structure function". Based on the precision inclusive cross section data, important progress could be reported to this conference in the quantitative investigation of deep inelastic diffraction.

2 Measurement of $F_2(x, Q^2)$

Since the inclusive deep inelastic scattering cross section

$$\frac{d\sigma}{dxdQ^2} = \frac{2\pi\alpha^2}{Q^4 x} \cdot [(2(1-y)+y^2)F_2(x,Q^2) - y^2 F_L(x,Q^2)] = \kappa \cdot F_2 \tag{1}$$

depends on two variables only, the measurement of the scattered electron energy E'_e and angle θ_e, of the hadronic quantity $\Sigma_h = \Sigma_i(E_i - p_i^z)$ and of the hadronic angle θ_h gives rise to an overconstrained determination of the kinematics and permits maximum coverage of the available (x, Q^2) range. Here y is the inelasticity variable, $y = Q^2/sx$, $s = 4E_eE_p$ with the beam energies $E_p = 820$ GeV and $E_e = 27.5$ GeV, and $\tan\ \theta_h/2 = \Sigma_h/p_T^h$ with $p_T^h = \sqrt{(\Sigma_i p_x^i)^2 + (\Sigma_i p_x^i)^2}$, where the summation extends over all particles but the scattered electron.

The F_2 structure function data presented to this conference [10, 14] was the last taken prior to the upgrade of the backward region of the H1 detector. Compared to previous analyses a new level of accuracy was achieved due to the larger statistics available for energy and angle calibrations and efficiency determinations. The measurement of E'_e could be calibrated to an absolute scale accuracy of 1% using the "kinematic peak shape" of the E'_e distribution, a cross section enhancement for $E'_e \simeq E_e$ at $x = E_e/E_p \simeq 0.03$, and the reconstruction of $E'_e = E(\theta_e, \theta_h)$ as functions of the two angles. The electron polar angle measurement was accurate to 1 mrad and the hadronic energy scale was known to 4%. An important error at lowest Q^2 was the uncertainty of the vertex reconstruction efficiency, up to 8% at large x and 4% at lowest x. The luminosity of 2.7 pb^{-1} was measured to 1.5% accuracy using the energy spectrum of hard photons ($E_\gamma \geq 10$ GeV) in the reaction $ep \to ep\gamma$. For the first time the H1 structure function measurement comprises data with a tagged, initial state radiated photon which enabled access

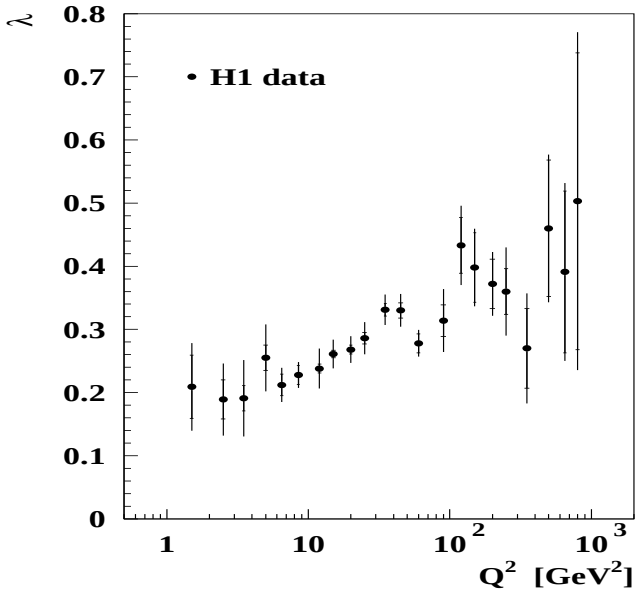


Figure 1: Derivative $\partial \ln F_2 / \partial \ln(1/x)$ determined in each Q^2 bin of the H1 data from a straight line fit to $\ln F_2 = a + \lambda \ln(1/x)$ with the full systematic error correlations taken into account. The inner error bar is the statistical error, the full error bar is the total error.

to the lowest Q^2 region due to the reduction of the incoming energy E_e by E_γ. The low Q^2 region was covered as well by data taken with a z vertex position shifted by +70 cm in proton beam direction which extended the measurement of F_2 to large values $\theta_e \leq 176.4^o$, θ being measured relatively to the proton beam direction. The accuracy at low $Q^2 \leq 8$ GeV^2 and at large $Q^2 \geq 80$ GeV^2 is only about 10 to 20% while in the region of the bulk data a systematic error down to 5% was achieved. Although this data is more precise than the previous one, it should be kept in mind that real precision measurements of $F_2(x, Q^2)$ with errors of about 2-3% in the whole kinematic range accessible by the HERA experiments are still to be performed [11].

The H1 measurement extends the knowledge of F_2 from fixed target lepton experiments by about two orders of magnitude towards lower x. A strong rise of F_2 is observed with decreasing x at fixed Q^2. This rise is correctly reproduced by a NLO QCD fit, described in [10], which starts from input gluon, sea and valence distributions at a chosen Q_o^2 value of 5 GeV^2 and generates that behaviour at larger and lower momentum transfers through the DGLAP evolution equations. The rise has been quantified by determining the exponent λ of $F_2 \propto x^{-\lambda}$ at fixed Q^2 using only the H1 data, see fig.1. So far this slope is determined rather precisely only for the intermediate Q^2 range between about 8 and 80 GeV^2. Note that there is a hidden possible x dependence of $\lambda(Q^2)$ since with rising Q^2 the mean x increases due to the y limitations of the kinematic region accessed, $\bar{Q}^2/\bar{x} \simeq 10^4$, roughly. If in the intermediate Q^2 range a common x interval between $x = 0.0008$ and $x = 0.008$ is chosen the dependence of λ on Q^2 gets slightly reduced. Higher precision data are needed, however, to contrast this with the expectation of a $1/\sqrt{ln(1/x)}$ dependence of λ on x.

The λ parameter not only quantifies the derivative of $\ln F_2$ vs $\ln(1/x)$ but is as well intimately connected with the behaviour of the photoproduction cross section because of $\sigma_{tot}(\gamma^* p) \propto F_2(W, Q^2)/Q^2$ where W is the energy in the $\gamma^* p$ centre of mass system, $W = \sqrt{Q^2/x} = \sqrt{sy}$ at low x. In the double logarithmic scaling hypothesis [15] which goes back to the roots of QCD [16] the distributions at low $Q^2 < M_p^2$ are soft, $F_2 \propto x^0$, and λ is expected to increase with Q^2, and to depend on x. As was discussed at this conference, the whole behaviour can be very well reproduced by an expression $\lambda \propto \sqrt{\ln T / \ln(1/x)}$ with $T = \ln(Q^2/\Lambda^2)/\ln(Q_o^2/\Lambda^2)$ [17]. In the alternative case of hard input or Pomeron distributions [18] one expects λ for the singlet distribution, which essentially is F_2 at low x, not to depend on Q^2 above some threshold value around 12 GeV^2. While the data seem to favour a Q^2 dependence of λ, reasonable fits have been obtained with a NLO factorization ansatz [18]. Improved precision at all Q^2 will finally settle this question which is an example of how intimately deep inelastic physics is related to its transition to the photoproduction region [19].

At low Q^2 the structure function data have been compared with various parametrizations of F_2, see fig.2. There are three observations to be emphasized: i) the data disfavour Regge based models for Q^2 larger than M_p^2; ii) the dynamical parton distributions of GRV [20] agree generally well with the measurement but have the tendency of overshooting the data at the lowest x values which may be cured by adjusting the starting point of the evolution and of Λ_{QCD}. The GRV approach is based on soft, valence like input distributions and thus fits to the double scaling concept; iii) various sets of global fits from CTEQ [21] and MRS [22], which use the 1993 or already the 1994 data, reproduce the behaviour of F_2. Of particular interest are the starting distributions which when considered at $Q^2 \simeq M_p^2$ seem to favour a soft singlet distribution as well.

The H1 collaboration has an ongoing long term programme for measuring F_2 with higher luminosity and an upgraded detector which should enable us to study the nature of quark-gluon

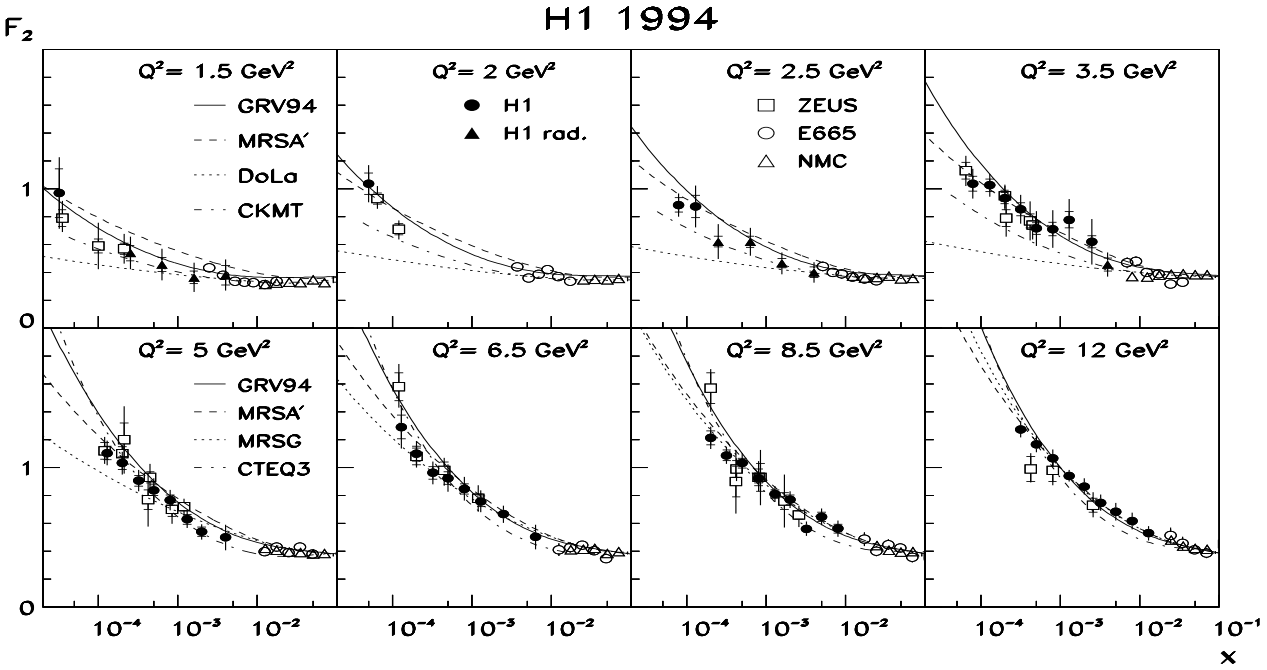


Figure 2: Measurement of F_2 at low Q^2 compared with ZEUS, E665 and NMC data and various structure function parametrizations.

interactions at high parton densities with F_2 much more precisely than so far. In particular, measurements with greater precision at lowest accessible x values in the DIS region may yet reveal BFKL interaction dynamics [23]. The prediction of the low x behaviour of F_2 according to BFKL still awaits the NLO calculations to be completed. Phenomenologically a unified treatment of DGLAP and BFKL dynamics is rather succesfull [24]. Interesting suggestions have been presented to search for BFKL dynamics in forward jet production [25] and E_T spectra [26] but no conclusive evidence has been established yet with the H1 data analyzed so far.

3 Access to the Gluon Distribution $xg(x, Q^2)$

3.1 Scaling Violations

Scaling is violated in any interacting field theory [27], logarithmically in QCD. The pattern of scaling violations has long ago been anticipated. At low x the structure function was predicted to increase with Q^2 due to quark pair production in the gluon field while at high x it should fall because of gluon radiation from quarks. Due to momentum conservation the integral of F_2 is about independent of Q^2 which leads to a turn over point at $x \simeq 0.13$ where scale invariance holds. This pattern is observed by H1 over a large range of x and Q^2 as can be seen in fig.3. The scaling violations for $x \leq 0.01$ determine directly the gluon distribution. In leading order perturbation theory one has approximately [28]

$$\frac{\partial F_2(x/2, Q^2)}{\partial \ln Q^2} \simeq \frac{10}{27} \frac{\alpha_s(Q^2)}{\pi} \cdot xg(x, Q^2) \tag{2}$$

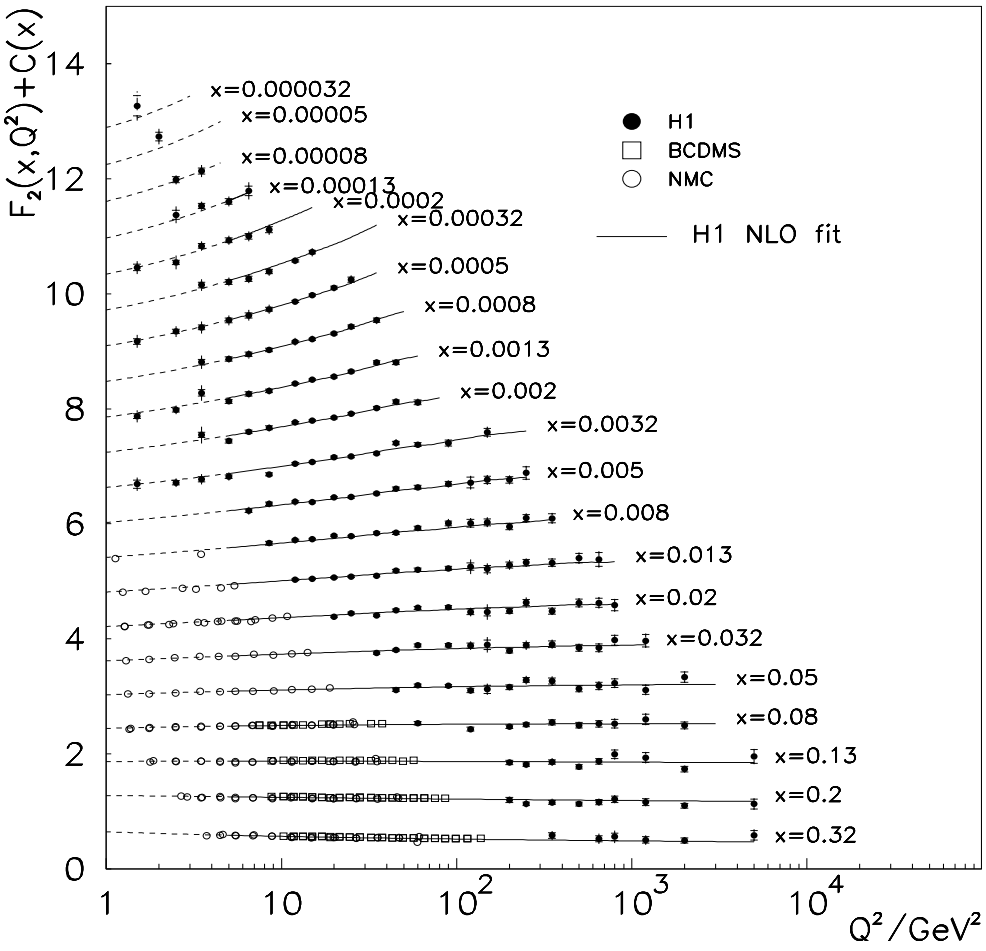


Figure 3: Dependence of $F_2(x, Q^2)$ on $\log Q^2$ as measured by the H1 experiment. The data is well described by a NLO QCD fit and smoothly extends the fixed target measurements into the higher Q^2 region albeit with less precision so far.

because the quark contribution to the derivative of F_2 is small ($\leq 10\%$) for $x < 0.01$.

The measurement of scaling violations is the most precise way to access the gluon distribution at low x. Fig.4 shows the result of a NLO QCD fit performed by H1 [10] using only F_2 structure function data. In this fit all parameters describing the singlet, gluon and valence quark distributions were fitted, the correlation of experimental systematic errors was considered and the QCD scale parameter Λ_{QCD} was fixed to 263 MeV. The gluon distribution rises towards low x the more the greater is Q^2. Such a behaviour is a result of the interaction dynamics as inherent in the DGLAP evolution equations. So far no deviation from this concept has been experimentally found in the behaviour of F_2 for $Q^2 \geq M_p^2$ at low x. Thus one may determine the gluon distribution at low x with this method down to Q^2 values around 1 GeV^2. This rather low Q^2 value phenomenologically may not be surprising: at low x the DGLAP equation for the gluon can be exactly solved [29, 18] leading to the behaviour

$$xg(x, Q^2) \propto \exp \sqrt{c \cdot \ln \frac{\ln(Q^2/\Lambda^2)}{\ln(Q_o^2/\Lambda^2)} \cdot \ln(1/x)}. \qquad (3)$$

This expression for $Q^2 \to Q_o^2$ degenerates to a normalization constant but it is still evolving with x and Q^2 even below 1 GeV^2 for Q_o^2 around 0.4 GeV^2, which is the GRV starting scale parameter and the value one can obtain by fitting a double logarithmic expression to the F_2 data [17].

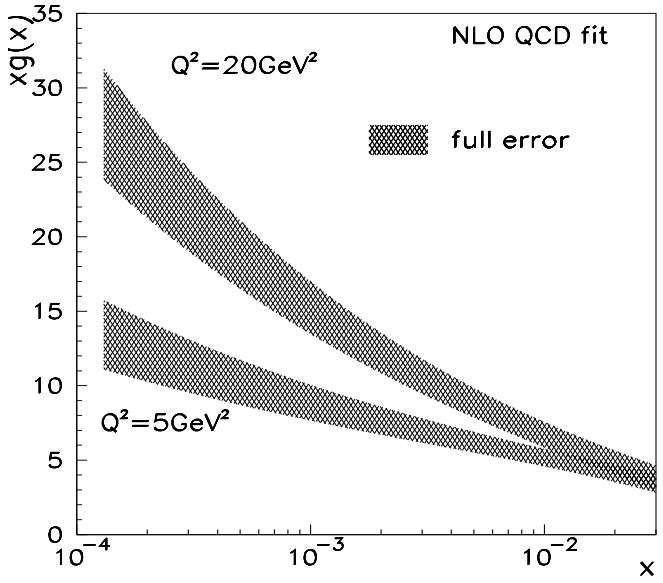


Figure 4: Gluon distribution determined by H1 from a NLO QCD fit to the H1, NMC and BCDMS proton and deuterium structure function data.

3.2 Longitudinal Structure Function $F_L(x, Q^2)$

In the quark-parton model the longitudinal structure function is zero for spin half quark-photon scattering [30]. In Quantum Chromodynamics F_L acquires a non zero value because of gluon radiation. At low x, as for $\partial F_2/\partial \ln Q^2$, the gluon distribution dominates which allows access to xg via the relation [31]

$$F_L = \frac{\alpha_s}{4\pi} x^2 \int \frac{dz}{z^3} \cdot [\frac{16}{3} F_2 + 8 \sum Q_q^2 (1 - \frac{x}{z}) g] \tag{4}$$

with the quark charges Q_q and written for four flavours, see [20] for the treatment of charm. The longitudinal structure function, together with F_2, allows an important consistency test of QCD, as eq.4 illustrates: at low x the gluon distribution determines simultaneously the scaling violations of F_2 and the size of F_L. F_L may differ by a factor of two in the BFKL approach [32, 33] from the DGLAP prediction and the predictions based on the factorization ansatz and on the double scaling hypothesis differ [18]. A measurement of F_L to about 10% precision is necessary to determine the behaviour of F_2 at the lowest x values which are accessible at high $y = Q^2/sx$. The H1 collaboration has presented a determination of F_L at low x to this conference for the first time [34]. At high $y \geq 0.6$ the y dependent weight factors of F_2 and F_L in eq.1 become of comparable size. Therefore the usual technique of extracting F_2 with a calculated F_L was reversed and F_L was determined after subtracting the F_2 contribution to

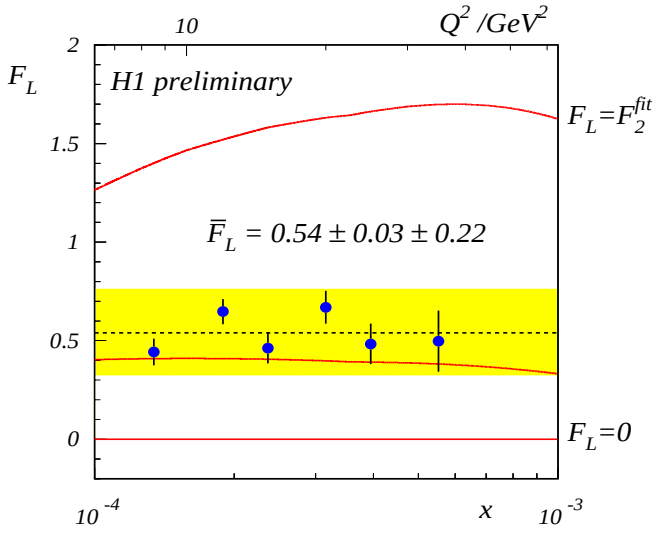


Figure 5: Measured longitudinal structure function F_L for $y = 0.7$ as functions of Q^2 and of $x = Q^2/sy$. The error bars are the statistical error, the band is the systematic error common to all points. The curve is a NLO QCD calculation of F_L using the gluon and quark distributions determined from the lower y H1 and BCDMS data.

the measured cross section. Contrary to the F_2 extraction which is based on *ad hoc* calculated values for F_L, this determination of F_L utilized the cross section measurement from a different y region which was extrapolated to high y in order to subtract the F_2 contribution. This extrapolation used a NLO QCD fit to F_2 performed in the lower y region.

The F_L measurement was performed using the most precise part of the 1994 data, for $7.5 < Q^2 < 42$ GeV^2, with a luminosity of 1.25 pb^{-1}. Access to F_L required the y range to be extended from a maximum of 0.6 [10] to 0.78, given by a reconstruction limit of the 1994 data placed near $E'_e = 6$ GeV. This was achieved using a lower energy calorimetric trigger combined with a central track trigger. A complete cross section reanalysis had to be performed which is in very good agreement with the published analysis.

The resulting longitudinal structure function is given in fig.5. It has been determined at six different x or Q^2 values for a common y value of 0.7. An average, preliminary value of $F_L = 0.54 \pm 0.03(stat) \pm 0.22(syst)$ has been determined at an average Q^2 value of 18 GeV^2 and $x = 0.0003$. The systematic error is mainly depending on y only. It includes both the measurement errors of the cross section at high y and the uncertainty of the subtracted F_2. That is due to the F_2 data errors at lower y, which partially get compensated, and to the fit procedure. On average the measured F_L value is 2.6 standard deviations larger than zero and 4 to 5 standard deviations away from F_2. With the specific values of F_2 and F_L as indicated in fig.5, $R = F_L/(F_2 - F_L)$ is about 0.5 with errors roughly 1.5 times larger than those of F_L. Compared to fixed target measurements at larger x values [35], R is rather large which is consistent with the gluon distribution at low x

The F_L extraction procedure assumes that F_2 follows NLO QCD. This is a reasonable assumption given the good agreement with QCD over many orders of magnitude in Q^2. Yet, it may not necessarily be true because one is exploring here at each Q^2 the lowest accessible x values where F_2 might depart from the expected behaviour. A measurement free of this

assumption requires the proton beam energy to be lowered which is an option planned in the HERA programme. Due to the reduced energy, however, this measurement will determine F_L values at about two times larger x at a given Q^2 than reachable with the subtraction method. At these higher x, for $Q^2 \geq 10$ GeV^2, the QCD description of F_2 is certainly valid. Yet, the comparison of the subtraction method with the result from two energy measurements will be very interesting for minimizing the systematic uncertainty of the F_L determination. At lower Q^2 the F_2 QCD extrapolation becomes questionable and the two energy measurements shall be essential in determining F_L.

3.3 Charm Structure Function

To leading order the charm structure function F_2^c is a direct measure of the gluon distribution because of the relation

$$F_2^c \;=\; \frac{Q^2\alpha_s(\mu^2)Q_c^2}{4\pi^2 m_c^2}\cdot\int_{x(1+4m_c^2/Q^2)}^{1}\frac{dz}{z}\cdot zg(z,\mu^2)\;C^{(0)} \tag{5}$$

with the scale parameter μ, the charm quark charge Q_c and mass m_c and the lowest order coefficient function $C^{(0)}$. At low x the quark contribution to the higher order expression [36] is small and the dependence of F_2^c on the renormalization and factorization scale is $\leq 10\%$ [37]. The measurement of the charm structure function allows an almost local determination of xg because at a given x the largest part of the integral stems from a narrow z interval. The H1

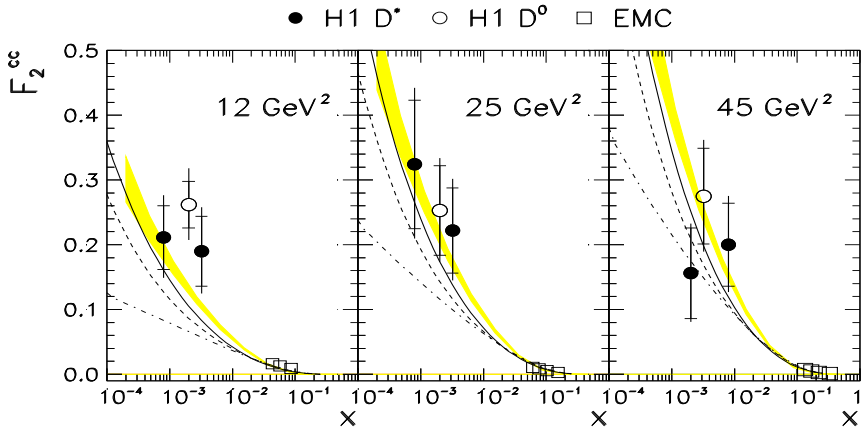


Figure 6: Measurement of F_2^c based on the observation of D^{*+} and D^0 production in deep inelastic ep scattering at low x. The full error bar represents the total error which is dominated by statistics (inner bars).

collaboration has presented preliminary data on F_2^c to this workshop [38]. The extraction of F_2^c relies on the observation of open charm production in deep inelastic scattering. Based on an integrated luminosity of 2.97 pb^{-1} 144 D^0 and 103 D^* events were found after statistical background subtraction in the $K\pi$ and the mass difference distribution, $m(D^*) - m(D^0)$, respectively. Taking into account the fragmentation function of $c \to D$ the D meson cross sections were determined and F_2^c was derived independently from both D meson data samples. The observed transverse momentum spectra of inclusive D^0 and D^* production were found to be

in good agreement with photon-gluon fusion calculations. The measured F_2^c is shown in fig.6 together with different NLO calculations of F_2^c. Remarkable agreement is observed between the measurement and the H1 calculation of F_2^c using essentially xg from the QCD fit to F_2 (dashed area in fig.6). The measurement extends the EMC data by two orders of magnitude down to $x \geq 0.0008$. Within the errors F_2^c does not depend on Q^2 and the ratio of F_2^c to F_2 is $0.237 \pm 0.021\ ^{+0.043}_{-0.039}$ at mean values of $Q^2 \simeq 26$ GeV^2 and $x \simeq 0.002$. A sizeable charm contribution to F_2 at low x could be expected from eq.5 because of the large gluon distribution.

The data presented are the first results on F_2^c from H1. With increased luminosity the charm structure function and the extraction of the gluon distribution will be of increasing importance with an expected precision of about 10% [39].

3.4 Elastic J/ψ Production

Results were presented by H1 on the deep inelastic and photoproduction of the vector mesons ρ, ω, Φ, ρ' and J/ψ based on data taken in 1994 with a luminosity of about 3 pb^{-1}. These provide an impressive amount of detailed information on the energy dependence and relative size of production cross sections, angular distributions and t dependence [40]. The J/ψ and ρ production have been selected here which provide some information on the gluon distribution.

Elastic J/ψ production has been viewed as proceeding via diffractive scattering [41] with a rather mild dependence of the cross section on W, the energy in the γp centre of mass system. In perturbative QCD, in leading order, the cross section for elastic J/ψ production is given by [42, 43]

$$\frac{d\sigma}{dt} = \frac{\Gamma_{ee} m_\psi^3 \pi^3}{48\alpha\mu^8} \cdot [\alpha_s(\mu^2) \cdot xg(x,\mu^2)]^2 \tag{6}$$

with $\mu^2 = m_\psi^2/4$ and $x = m_\psi^2/W^2$, i.e. it is a direct measure of the gluon distribution with m_ψ providing the hard scale [44]. The energy dependence of the J/ψ production cross section is related to the low x behaviour of the gluon density and expected to be rather steep. Elastic

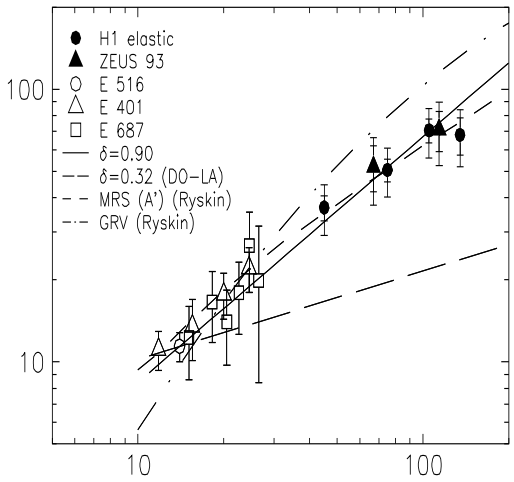


Figure 7: Total cross section for elastic J/ψ photoproduction versus the cms energy of the γp system. The inner error bars of the H1 data points are the statistical error, the full error bar represents the total error.

J/ψ events have been analyzed [40, 45] in four intervals of W in $J/\psi \to \mu^+\mu^-$ with 2.7 pb^{-1} (233 events) and in $J/\psi \to e^+e^-$ with 2.0 pb^{-1}(165 events) using a set of five different triggers sensitive to charged lepton production. Nearly background free J/ψ samples were selected with a reconstructed mass of 3.10 ± 0.01 GeV ($\mu\mu$) and 3.08 ± 0.02 GeV (ee) to be compared with the PDG value of $m_\psi = 3.097$ GeV. Fig.7 illustrates the W dependence of the measured cross section. A parametrization of $\sigma \propto W^\delta$ clearly favours a strong W dependence with $\delta \simeq 0.9$ over the diffractive hypothesis with δ between 0.22 and 0.32. This trend is observed with the large J/ψ production cross section measured at W around 100 GeV as compared to previous fixed target experiments but it is as well consistent with the W dependence established by the H1 data alone. The energy dependence of the cross section can be well described by the model [42] with the MRSA' gluon parametrization which behaves like $x^{-0.2}$ at low x.

Data were presented also on inelastic J/ψ photoproduction [40, 45], about 85 events with a J/ψ decay into $\mu^+\mu^-$, which are in good agreement with NLO QCD calculations [46] both in normalization and energy dependence. Yet, reliable predictions were obtained only for inelasticity values $z = y_\psi/y \leq 0.8$ and transverse momenta $P_T^\psi \geq 1$ GeV. This cuts into the low x region reducing the data by about one half and thereby the sensitivity of the cross section to the still possible variations of the gluon density. Nevertheless, this process may provide a rather precise determination of xg but unlikely at the smallest x accessible by the data.

3.5 Elastic ρ^o Production

Deep inelastic ρ production is another process sensitive to the gluon distribution with a cross section for longitudinally polarized photons of

$$\frac{d\sigma}{dt} \propto \frac{[\alpha_s(\mu^2) \cdot xg(x,\mu^2)]^2}{Q^6} \cdot C_\rho. \tag{7}$$

The situation is similar to J/ψ production with a predicted weak W dependence in diffractive models [41] and a stronger rise expected in QCD. Yet, for ρ (and ϕ) production it requires a large virtuality of the process to introduce a hard scale. Another expectation from eq.7 is a Q^2 dependence of Q^{-2n} with $n \simeq 2.5$ since at low x $(\alpha_s xg)^2 \propto \sqrt{Q^2}$ and C_ρ only weakly depends on Q^2 [50]. Fig.8 summarizes the elastic cross section measurements of ρ photoproduction [47] and large Q^2 production [48]. The ρ decay pions were reconstructed in the central drift chambers apart from photoproduction data at $W \simeq 200$ GeV which had to use a calorimetric measurement because of the large boost of the ρ^o rest frame which forced the pions outside the tracker acceptance region. At $Q^2 \simeq 10$ GeV^2 104 events were analyzed and at $Q^2 \simeq 20$ GeV^2 78 events from a luminosity of 2.8 pb^{-1}. The result is somewhat lower than the ZEUS data which have a 31% normalization uncertainty [49] not drawn in fig.8. A combination of the H1 results with the NMC data reveals an increase of the cross section $\propto W^\delta$ with $\delta = 0.56 \pm 0.20$ at $Q^2 = 10$ GeV^2 and $\delta = 0.40 \pm 0.24$ at $Q^2 = 20$ GeV^2. The error includes the uncertainties of both experiments. The photoproduction cross section, however, does not depend strongly on W which differs from the J/ψ result. The Q^2 dependence has been measured and $n = 2.5 \pm 0.5 \pm 0.2$ obtained with a dominant statistical error. These results support the QCD approach to deep inelastic ρ production and are consistent with expectations from the behaviour of the gluon distribution at low x. It remains to be seen whether future more precise data and the quantitative understanding of non-perturbative effects [50, 51] lead to a consistent picture of this interesting process.

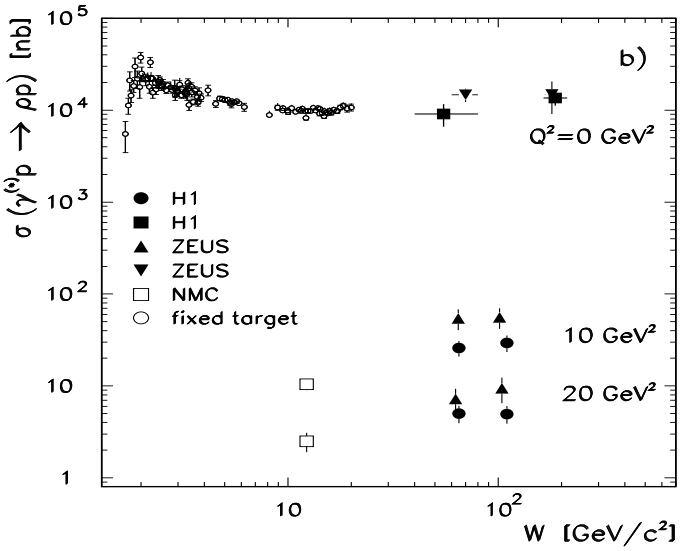


Figure 8: Total cross section for elastic ρ production versus the cms energy of the γp system compared with ZEUS and fixed target data.

3.6 Jets in Deep Inelastic Scattering

While gluons had not been 'seen' yet, the CHEEP proposal [2] anticipated the existence of three jet events in deep inelastic scattering with a cross section written as the sum of photon-gluon fusion (σ_{pgf}) and Compton scattering (σ_{com}) contributions [52] as

$$\sigma_{jet} = \alpha_s(Q^2) \int \frac{dx}{x}[xg(x,Q^2) \cdot \sigma_{pgf} + \sum_q xq(x,Q^2) \cdot \sigma_{com}]. \quad (8)$$

Here three jets actually denote the proton remnant centered around the beam line and the two quark jets or a quark and a gluon jet. To leading order one has calculated and corrected for the Compton contribution, identified x with $x_{Bj}(1+m^2/Q^2)$, m being the two jet mass, and unfolded directly the gluon distribution with some assumption on α_s [53]. The H1 Collaboration has presented a NLO extension of this approach to this conference [54] which required to replace the direct unfolding by a fitting procedure solving the cross section integrals with a Mellin transformation technique [55]. Four values of the measured relative rate of three jet events for Q^2 between 40 and 4000 GeV^2 were used as observables. The fit procedure resembles the structure function QCD analysis as an assumption $xg = ax^b \cdot (1-x)^c(1+dx)$ was made at $Q_o^2 = 4$ GeV^2 and the gluon distribution obtained through the QCD evolution at higher Q^2. Fig.9 represents the first gluon distribution determined by H1 from DIS jet production analyzed in NLO for $x \geq y_c$ where y_c is the minimum resolution parameter in the JADE jet finding algorithm applied here [56]. The jet formation was simulated to NLO using the PROJET program [57] and the transition of the observation from the jet to the parton level was done using LEPTO [58]. The result is in good agreement with the standard gluon parametrizations and the method promises for a more accurate gluon determination at HERA in the deep inelastic regime for $x > y_c \simeq 0.02$.

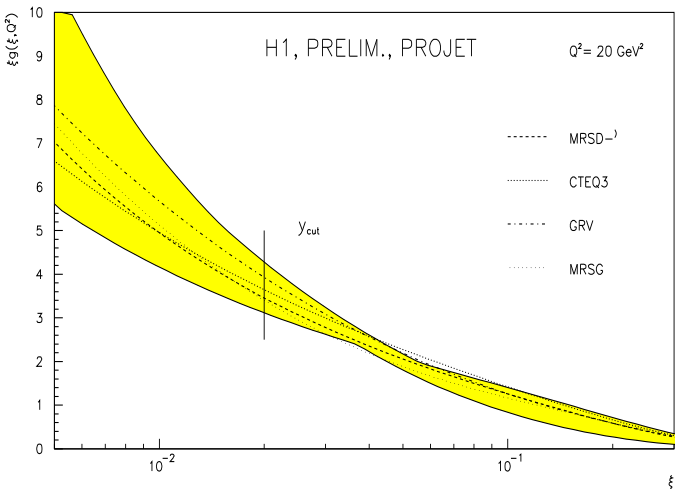


Figure 9: The gluon density obtained from DIS three jet production compared to standard gluon parametrizations based on structure function and direct photon data. The band represents the analysis uncertainty.

4 The Strong Coupling Constant $\alpha_s(Q^2)$

4.1 $\alpha_s(Q^2)$ from Jets

The relative three jet rate R_{2+1} has long been viewed as a way to measure $\alpha_s(Q^2)$. A theoretical and practical complication of this α_s determination is due to the fact that hadrons are observed instead of partons and that the jet definition remains to be ambiguous to some extent. Shortly before the Rome conference a new NLO jet simulation program, MEPJET [59], became available which allows tuning the program to any of the different procedures of jet recombination. This is promising as it ensures a very similar treatment of data and simulation. The H1 Collaboration presented a progress report [54] on the determination of $\alpha_s(M_Z^2)$ for different recombination schemes using the PROJET and the MEPJET code. In MEPJET there is a reduced dependence of the α_s values on the recombination algorithm. The central value in the 'E' scheme comes out to be around 0.112 instead of 0.127 using PROJET. This is mainly due to a decrease of the measured α_s value at the lowest $Q^2 \simeq 200$ GeV^2 where the neglect of terms $\propto y_c W^2$ in PROJET becomes relevant.

At the present stage of the analysis this α_s determination has systematic errors of about 0.010 [60] due to a hadronic energy measurement scale error of 4%, to hadronization and parton density uncertainties, statistics, scale and y_c effects. Further understanding of the whole procedure and an increase of the luminosity giving access to the highest Q^2 region should permit a substantial reduction in this uncertainty.

4.2 QCD Analysis of Scaling Violations

The classical method to determine the strong coupling constant in deep inelastic scattering has been to investigate the scaling violations of $F_2(x, Q^2)$ which lead to $\alpha_s(M_z^2) = 0.113 \pm$

0.005 [61] based on the BCDMS and SLAC experiments. The distinction between the gluon distribution and α_s is practically difficult because whenever xg appears in the expression for a cross section it is naturally multiplied with α_s which, however, has a unique Q^2 dependence. The BCDMS/SLAC value was determined using data at rather large x where the contribution of the gluon distribution to the QCD F_2 evolution equation is small. Loosely speaking it is a value determined from gluon bremsstrahlung rather than quark pair production from gluons. The latter dominates at HERA.

The H1 Collaboration has not yet presented an α_s determination based on the NLO QCD description of its structure function data. There is sensitivity but Λ_{QCD} is correlated to some of the many fit parameters and improved precision of the F_2 data in the full kinematic range is desirable. In [62] α_s was determined from the 1993 H1 data by fixing the high x parameters using global fits. A central value of 0.120 was obtained which is also somewhat favoured over 0.113 in a recent global analysis including the Fermilab jet data [22].

The H1 Collaboration has shown that double logarithmic scaling [62] in combinations of the variables $\ln(x_o/x)$ and $\ln(\alpha_s(Q_0^2)/\alpha_s(Q^2))$ holds to some approximation [10]. This assumption has been used and a reanalysis was made which determined $\alpha_s(M_Z^2)$ to $0.113 \pm 0.002 \pm 0.006$ [17] using the 1994 F_2 H1 data only. The advantage and the difficulty of this approach is that here xg and α_s appear to be decoupled: the gluon distribution is not entering anymore as it is essentially determined through eq.3. This approach perhaps will permit a rather precise α_s determination if double logarithmic scaling continues to be supported by F_2 precision data and if the theoretical approximations can be better understood.

The α_s determinations have a remarkable theoretical uncertainty due to factorization and renormalization scale uncertainties which were reconsidered recently [63]. NNLO calculations of the splitting functions seem to be unavoidable for matching the envisaged experimental precision of $\alpha_s(M_Z^2)$ at HERA of $\simeq 0.002$ [11].

5 Weak Charged Currents

Charged current events in H1 have the spectacular signature of a hadronic system of large transverse momentum, $p_T^2 = Q^2(1-y)$, which remains unbalanced as the (anti)neutrino escapes detection. Based on a luminosity of 2.7 pb^{-1} for 1994 and 3.7 pb^{-1} for 1995 25 e^- and 105 e^+ induced charged current events were measured with $p_T > 25$ GeV. The kinematics are reconstructed using the Σ method [64]. Background is efficiently removed with vertex, event topology and calorimeter timing requirements. Details of the analysis are described in [65]. Despite the limited statistics three basic observations were made: i) at $Q^2 \simeq G_F/\sqrt{2}e^2$ the neutral and charged current inclusive cross sections become of similar size, see [65]; ii) since HERA is equivalent to a 50 TeV neutrino beam fixed target experiment, H1 was able to discover departures from the linear energy dependence of the cross section with a measured propagator mass of $m_W = 84\ ^{+9}_{-6}\ ^{+5}_{-4}$ GeV in agreement with the most precise W mass measurements at the Tevatron; iii) the W boson can be used to probe the proton structure at very large Q^2. A first measurement of the x distribution in charged current positron scattering, still not bin size corrected, is shown in fig.10. The result is somewhat higher than the calculated cross section extrapolating the MRSH distributions to the high Q^2 region. Higher luminosity will permit access to the valence quark region and to a measurement of the up and down quark proton contents. As has been demonstrated 10 years ago [66], HERA may permit the determination of

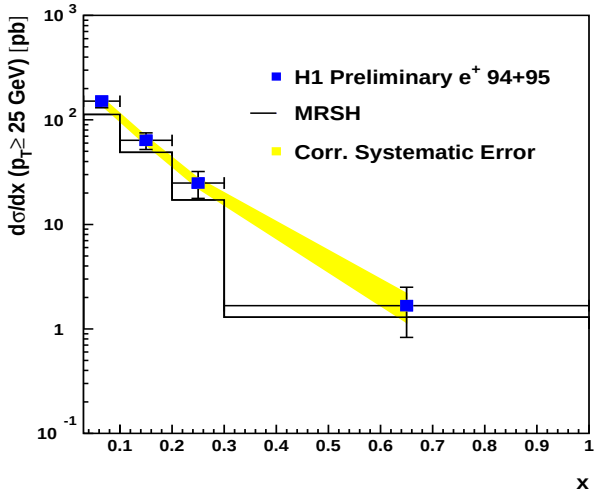


Figure 10: Weak charged current cross sections measured by H1 as a function of x.

the electroweak mixing angle $\sin^2\theta$ with a precision of about 0.002 using the neutral to charged current cross section ratio in e^- scattering. This will be an interesting consistency test of the electroweak theory performed in the spacelike region.

6 Deep Inelastic Diffraction

A new experimental and QCD analysis of diffractive deep inelastic scattering was presented by H1 [67] based on about 20,000 events obtained for $2.5 \leq Q^2 \leq 65$ GeV^2 with a luminosity of 2.0 pb^{-1} collected in 1994. The event selection criteria have been very similar to the inclusive F_2 analysis adding the requirement of a gap in the pseudo-rapidity range $3.0 < \eta < 7.5$ which restricts the proton remnant mass to $M_Y < 1.6$ GeV. The exchanged object ('pomeron') carries a fraction $x_{I\!P}$ of the pomeron momentum in the proton measured as $x_{I\!P} = x \cdot (Q^2 + M_X^2)/Q^2$ where M_X^2 is the mass of the hadronic system produced with the rapidity gap $\Delta\eta$ to the proton or its dissociation product. In the partonic view of the $I\!P$ there are quarks and gluons with a fraction β of the pomeron momentum, i.e. $\beta = x/x_{I\!P} = Q^2/(Q^2 + M_X^2)$. The mass M_X is measured with the calorimeter cell energies in appropriate combination with reconstructed tracks and Q^2 and x are determined with the Σ method.

Fig.11 shows the measurement of the structure function [68] $F_2^{D(3)}(\beta, Q^2, x_{I\!P})$ extracted from the triple differential cross section divided by the kinematic factor κ, eq.1, for $F_L = 0$ integrating over $-t < 1$ GeV^2 where t is the yet unmeasured momentum transfer from the proton to the M_X system. The structure function is well described by a fit $F_2^{D(3)}(\beta, Q^2, x_{I\!P}) = A(\beta, Q^2) \cdot x_{I\!P}^{-n}$. This measurement established a dependence of n on β for $\beta \leq 0.3$ which implies that simple factorization of the deep inelastic diffractive cross section into a universal flux factor and a structure function $A \propto F_2^D$ does not hold. This may be due to an exchange of more than a single Regge trajectory [69]. Apart from the lowest β the measured n values, fig.11, are still not far from their naive expectation value of $n = 2\alpha(0) - 1 \simeq 1.17$ introducing the pomeron Regge trajectory with an intercept of about 1.085 as derived from soft hadron diffraction experiments.

Integrating $F_2^{3(D)}$ over $x_{I\!P}$ from 0.0003 to 0.05, i.e. considering all accessed momenta of the pomeron in the proton, H1 obtained the structure function $\tilde{F}_2^D$ which rises with Q^2 up

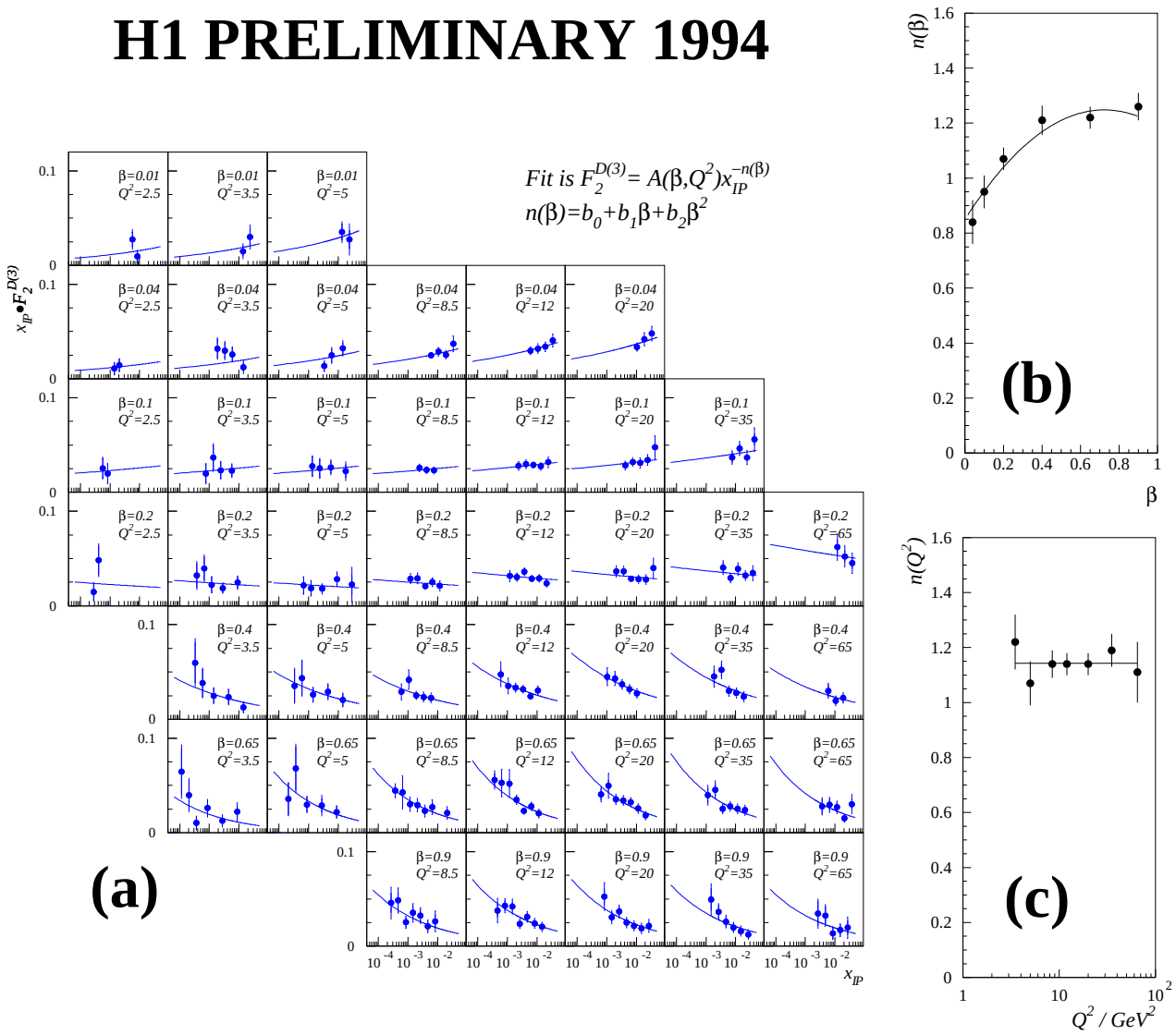


Figure 11: (a) $x_{I\!P} \cdot F_2^{D(3)}(\beta, Q^2, x_{I\!P})$ as measured by H1 and the β (b) and Q^2 (c) dependence of n determined from fits $F_2^{D(3)} = A(\beta, Q^2)/{x_{I\!P}}^n$. The experimental errors are statistical and systematic added in quadrature. The fit described in the text is shown.

to β near 0.9 but does not depend on β in the covered Q^2 range [67]. This can be explained with gluon dominance in the pomeron up to largest β in an appealing attempt to quantify the Q^2, β behaviour of $\tilde{F}_2^D$ in a DGLAP evolution approach. For Q^2 between 2 and 70 GeV^2 the gluon carries 90 to 80% of the pomeron momentum, respectively. This is consistent with the experimental observation of diffractive D^* production and the study of energy flow in the $\gamma^* I\!P$ cms [70]: central particle production is observed as expected from a three parton 'final' state, e.g. from two quarks from photon-gluon fusion and a radiated second gluon. A quark object would predominantly produce two partons giving rise to particle production aligned with the $\gamma^* I\!P$ axis, contrary to what is observed experimentally. The diffractive structure function measurement is as well consistent with diffractive jet production [71] and event shape analyses [72]. The systematic errors of $F_2^{D(3)}$ are still about 20% due to energy scale errors and simulation uncertainties. A precise investigation of diffraction at HERA is still ahead.

7 Concluding Remarks

The results presented by H1 to the 1996 DIS conference represent an impressive extension of the physics scope as compared to the previous DIS conference [73] with a first rather precise F_2 measurement, the first F_L and F_2^c determinations, the first NLO gluon distribution determined from jets, the proton structure probed with W bosons, apparently broken factorization of the deep inelastic diffraction cross section and further interesting observations. It can steadily be anticipated how impressive the physics at HERA will be in 2005, at a machine which by then represents a 30 years long dream and effort to investigate with an electron-proton collider the substructure of matter and the unification of forces by gauge field theories. It is likely to be precision which at HERA leads to new insight requiring luminosity and patience.

Acknowledgment The results presented here are due to a huge, collaborative effort of too many people to be named here. I wish to express special thanks to all members of the Zeuthen H1 group for their friendly support over the lifetime of H1, the H1 structure function group for intense joint work over the last years and the Rome speakers of H1 for sharing their expertise and for their generosity when I failed to include their favoured results into this presentation. My attempt to summarize the deep inelastic physics of H1 would not have been undertaken without the advice and encouragement of John Dainton, Albert DeRoeck, Ralph Eichler and Joel Feltesse. Thanks are due to Guilio D'Agostini and his team for organizing a remarkable conference in Rome, and to Andrea Nigro for a very friendly approach towards completion of this writeup. I finally thank the former minister of science and education of Italy, our colleague Giorgio Salvini, for making me think harder about the past and the success of the deep inelastic physics research at HERA.

References

[1] H.D. Politzer, Phys.Rep. **C 14** (1974) 129.

[2] *CHEEP - An ep Facility in the SPS*, J.Ellis, B.H.Wiik and K.Hübner, eds., CERN yellow report 78-02(1978).

[3] SLAC: C.Pellegrini et al., Proc. 8th Int.Accelerator Conf., CERN, 1971, p.153.
DESY: H.Gerke et al., DESY H-72/22(1972).

[4] R.P. Feynman, Phys.Rev.Lett. **23** (1969) 1415.
J.D. Bjorken and E.A. Paschos, Phys.Rev. **158** (1969) 1975.

[5] R.P. Feynman, Photon-Hadron Interactions, Benjamin, New York, 1972.

[6] J. Ellis, in [2], p.9.

[7] I. Abt et al., H1 Collaboration, Nucl.Instr. Methods to appear.

[8] J. Ellis, Proc.for European *ep* Facility, ed. U. Amaldi, DESY 79-48(1979).
R.P. Feynman, in [5], p.344.

[9] F. Eisele, Proc.Europhysics Conf., Brussels, DESY 95-229 (1995).
A. Caldwell, Proc. Int. Lepton-Photon Symposium, Beijing, DESY 95-231 (1995).

[10] H1 Collaboration, S. Aid et al., Nucl.Phys. **B 490** (1996) 3.

[11] M. Botje, M. Klein and C. Pascaud, *Precision Measurements of F_2, α_s and xg at HERA* , Proc. HERA Workshop, Hamburg 1996 (Proc. HERA96), ed. by A. DeRoeck, G. Ingelman and R. Klanner, to be published.

[12] Yu. L. Dokshitzer, Sov. Phys. JETP **46** (1977) 641.
V. N. Gribov and L.N. Lipatov, Sov. J. Nucl. Phys. **15** (1972) 438 and 675.
G. Altarelli and G. Parisi, Nucl.Phys. **B 126** (1977) 298.

[13] A. Donnachie and P.V. Landshoff, Proc. HERA Workshop Hamburg 1987 (Proc. HERA87), ed. by R. Peccei, Vol.1, p.351 and CERN-Th.5020/88(1988).

[14] U. Bassler, H1 Collaboration, Proc. Int. Workshop on Deep Inelastic Scattering and QCD, Rome (1996), subsequently termed "these proceedings".

[15] R. Ball and S. Forte, Phys.Lett. **B 335** (1994) 77.

[16] A. DeRùjula et al., Phys.Rev. **D 10** (1974) 1649.

[17] A. DeRoeck, M. Klein and T. Naumann, DESY 96-063(1996), Phys.Lett. to appear; T.Naumann, these proceedings.

[18] F.J. Ynduráin, FTUAM 96-12(1996), August 1996.

[19] see e.g. A. Levy, DESY 95-204(1995) and these proceedings.

[20] M. Glück, E. Reya and A. Vogt, Z.Phys. **C 67** (1995) 433.
A. Vogt, Proc. Int. Workshop on Deep Inelastic Scattering and QCD, Paris (1995) ed by V. Brisson, p.261.

[21] CTEQ Collaboration, J. Botts et al., Phys.Lett. **B 304** (1993) 15.

[22] A.D. Martin, R.G. Roberts and W.J. Stirling, RAL-TR-96-037(1996).

[23] E.A. Kuraev, L.N. Lipatov and V.S. Fadin, Sov.Phys. JETP **45**(1977)199.
Y.Y. Balitsky and L.N. Lipatov, Sov.J.Nucl.Phys. **28**(1978)822.

[24] J. Kwiecinski, A.D. Martin and P.J. Sutton, DTP/96/02(1996).
A.D. Martin, these proceedings.

[25] S. Aid et al., H1 Collaboration, Phys.Lett. **B 356** (1995) 118.
A. DeRoeck, these proceedings.

[26] M. Kuhlen, these proceedings and MPI-PhE/96-10(1996).

[27] S. Coleman and D.J. Gross, Phys.Rev.Lett. **59** (1973) 851.

[28] K. Prytz, Phys.Lett. **B 311** (1993) 286.

[29] A. Mueller, Nucl.Phys.B:Proc.Suppl. **29A** (1992) 275.

[30] C. Callan and D.J. Gross, Phys.Rev.Lett. **22** (1969) 156.

[31] A. Zee, F. Wilczek and S.B. Treiman, Phys.Rev. **D 10** (1974) 2881.
G. Altarelli and G. Martinelli, Phys.Lett. **B 76** (1978) 89.

[32] R. Peschanski and G.P. Salam, *The QCD Dipole Picture of Small x Physics*, Proc. HERA96.

[33] R. Ball, these proceedings.

[34] M. Klein, H1 Collaboration, these proceedings.

[35] A. Milstaijn, NMC Collaboration,these proceedings.

[36] S. Riemersma et al., Phys.Lett. **B 347** (1995) 143.

[37] B. Badelek et al., J.Phys.G: Nucl.Part.Phys. **22** (1996) 815.

[38] K. Daum, H1 Collaboration, these proceedings.

[39] K. Daum, *Future F_2^c Measurements at HERA*, Proc. HERA96.

[40] B. Clerbaux, H1 Collaboration, these proceedings.
S. Schiek and G. Schmidt, H1 Collaboration, these proceedings.
for strangeness production see K. Johannsen, H1 Collaboration, these proceedings.

[41] A. Donnachie and P. Landshoff, Phys.Lett. **B 348** (1995) 213.

[42] M.G. Ryskin, Z.Phys. **C 57** (1993) 89.
see M.G. Ryskin et al., Durham and RAL preprints, hep-ph/9511228 (1995).

[43] S.J. Brodsky et al., Phys.Rev. **D 50** (1994) 3134.

[44] L. Frankfurt and A. Levy, J.Phys.G: Nucl.Part.Phys. **22** (1996) 873.

[45] S.Aid et al., H1 Collaboration, Nucl.Phys. **B 472** (1996) 3.

[46] M. Krämer, Nucl.Phys. **B 459** (1996) 3.

[47] S.Aid et al., H1 Collaboration, Nucl.Phys. **B 463** (1996) 3.

[48] S.Aid et al., H1 Collaboration, DESY 96-023(1996), Nucl.Phys. to appear.

[49] M. Derrick et al., ZEUS Collaboration, Nucl.Phys. **B 356** (1995) 901.

[50] L. Frankfurt, W. Koepf and M. Strikhman, TAUP 2290-95 (1995).

[51] B.Z. Kopelovitch et al., Phys.Lett. **B 324** (1994) 469.
H. Abramowicz, L. Frankfurt and M. Strikhman, DESY 95-047(1995).

[52] H. Georgi and H.D. Politzer, HUTP 77/A063 (1977).
A. Mendez, Nucl.Phys. **B 145** (1978) 199.

[53] S.Aid et al., H1 Collaboration, Nucl.Phys. **B 449** (1995) 3.

[54] K. Rosenbauer, H1 Collaboration, these proceedings.
see also K. Flamm, H1 Collaboration, these proceedings.

[55] D. Graudenz et al., Z.Phys. **C 70** (1996) 770.

[56] W. Bartel et al., JADE Collaboration, Z.Phys. **C 33** (1986) 23.

[57] D. Graudenz, PROJET 4.1, CERN-Th 7420/94 (1994).

[58] G. Ingelman, LEPTO 6.3 program manual, unpublished.

[59] E. Mirkes and D. Zeppenfeld, Phys.Lett. **B 380** (1996) 105 and these proceedings.

[60] M. Jaffre, H1 Collaboration, Proc. La Thuille, 1996, to be published.

[61] A. Milstaijn and M. Virchaux, Phys.Lett. **B 274** (1992) 221.

[62] R. Ball and S. Forte, Phys.Lett. **B 358** (1995) 365.

[63] J. Blümlein et al., *Theoretical Uncertainties in the QCD Evolution of Structure Functions and their Impact on* α_s, Proc. HERA96.

[64] U. Bassler and G. Bernardi, Nucl. Instr. Meth. **A361** (1995) 197.

[65] S. Aid et al. H1 Collaboration, Z.Phys. **C 67** (1995) 565.
S. Aid et al. H1 Collaboration, DESY 96-01(1996).
A. Pieuchot, H1 Collaboration, these proceedings.

[66] J. Blümlein, M. Klein and T. Riemann, Proc. HERA87 Vol.2, p.687.

[67] P.R. Newman, these proceedings.

[68] G. Ingelman and P. Schlein, Phys.Lett. **B 152** (1985) 256.

[69] P. Landshoff, these proceedings.

[70] S. Tapprogge, H1 Collaboration, these proceedings.
A. Mehta, Proc. Diffr. Conf., Eilat 1996, ed. by H. Abramowicz and A. Levy.

[71] J. Theissen, H1 Collaboration, these proceedings.

[72] A. Valkarova, H1 Collaboration, these proceedings.

[73] J. Dainton, H1 Collaboration, Proc.Int.Conf. DIS, Paris, 1995, p.37, ed by V. Brisson.